Research Journal of Engineering Sciences ___________________________________ ISSN 2278 – 9472
Vol. **10(3),** 13-18, September **(2021)** *Res. J. Engineering Sci.*

Effect of mechanical parameter variations in BLDC motor drive

Juli Singh Sadhak[1*], Surekha Bhusnur[2], S.P. Dubey[3] and Amit Sadhak[4]
[1]Electrical Engg. Department, BIT Durg, Chhattisgarh, India
[2]EEE Department, BIT Durg, Chhattisgarh, India
[3]MATS Raipur Chhattisgarh, India
[4]Electrical Engg., R.C.E.T. Bhilai, Chhattisgarh, India
singh.juli@gmail.com

Available online at: www.isca.in, www.isca.me
Received 18th November 2020, revised 8th August 2021, accepted 23rd September 2021

Abstract

The electrical machines with a scheme of Controlled motion is known as electric-drives. With the implementation of drive we can achieve Specific control for speed of an electrical-machine. Optimization is easily feasible for control of motor motion via drive. A drive comprises of electric machine with power electronic, with converter controllers. Recent advanced practises have paved the way development of more trustworthy, proficient, & reduction in sizes, Alternating Current and Direct Current motor drives. According to this paper it executes the most popular motor i.e. BLDC motor. In this research paper we have mathematically designed PMBLDC Motor with analysis of their simulation performance with the help of coding in MATLAB is done. In this paper we have simulate with the aid of coding the output analysis of operation of PM BLDC motor via MATLAB (R2016a) version. The BLDC motor drive scheme is yet one of omnipresent research troubles.

Keywords: PM BLDC – Permanent Magnet Brushless D.C. Motor, EMF- Electro Magnetic force, BEMF- Back Electro Magnetic force.

Introduction

When Permanent Magnet Synchronous Motors have induced EMF trapezoidal in shape then it is known as Permanent Magnet Brushless Direct Current Machines (PMBDCM). As compared to its equivalent, success of these machineslies on its simple control. The current commutation is started in any of the phase of machine when the constant flat portion of the induced back EMF has started or has ended[1].

Drives being coded to ensure that system posses more efficiency, is fault tolerant, has quieter operation, smaller size for many different applications. Modeling and design tools are being developed so that there is reduction in efforts for drive development and designing of machine. Dedicated researches are focused on reluctance type machines drives and permanent magnet machine drives[1]. These motors have very prevalent industrial applications as their construction fits for any safety required applications.

BLDC motors are supplied by a traditional 3-ϕcontrolled inverter. Normally rotor position sensor increases cost, size, weight and complexity of control thereby reducing the dependability and tolerability of these drives. Motor with controller are very costly hence very few marketable applications of sensorless BLDC motor are present.

So this method is normally adapted for much application like fan, pump, computer equipments as hard drives. Heating and ventilation, Laser printer, AC and DC power supplies, Brushless DC Motors used in Medical Treatment 1. Treating Sleep Apnoea, 2.Motors in Hospital Equipment, 3.Medical Analyzers, 4.Optimizing Power Density applications which doesn't have large torque variety during starting and normalrunning[2].

Modelling of PM Brushless DC Motor Sensorless Technique

Here motor is taken as3-ϕ even though the derivation is applicable for more number of phases[3]. The stator winding equations based on coupled elements for constants terms of motorare

$$\begin{bmatrix} v_{ast} \\ v_{bst} \\ v_{cst} \end{bmatrix} = \begin{bmatrix} R_s & 0 & 0 \\ 0 & R_s & 0 \\ 0 & 0 & R_s \end{bmatrix} \begin{bmatrix} i_{ast} \\ i_{bst} \\ i_{cst} \end{bmatrix} + \begin{bmatrix} (L_s - M) & 0 & 0 \\ 0 & (L_s - M) & 0 \\ 0 & 0 & (L_s - M) \end{bmatrix} \frac{d}{dt} \begin{bmatrix} i_{ast} \\ i_{bst} \\ i_{cst} \end{bmatrix} + \begin{bmatrix} e_{ast} \\ e_{bst} \\ e_{cst} \end{bmatrix} \quad (1)$$

Where R_s is resistance/ phase of stator winding, which are taken as equal for 3- phases. The induced EMFs e_{ast}, e_{bst}, and e_{cst} all are assumed to be trapezoidal. E_p is the max EMF value which is derived as

$$E_p = (Blv)N = N(Blr\omega_m) = N\varphi a\omega_{rs} = \lambda_p\omega_{rs} \quad (2)$$

Where, the total conductors connected in series/phase =N, rotor, Velocity(m/s) =v, Conductors length(m) = l, Rotor radius(m) = r, Angular velocity(rad/s) =ω_{rs}, Conductors flux density (Tesla) =B are placed[3].

The voltage equation of phase is similar to voltage equation of armature of Direct Current machine. This is due to the fact that it is quite similar to D.C. machine except brushes and commutator being removed, hence the name of machine as Permanent Magnet Brushless dcmachine[3]. The electromagnetic torque (T_e) equation is

$$T_e = [e_{ast} i_{ast} + e_{bst} i_{bst} + e_{cst} i_{cst}] \frac{1}{\omega_{rs}} (N \cdot m)$$
(3)

The instantaneous-induced EMFs is given as

$$e_{ast} = f_{ast}(\theta_{ra}) \lambda_p \omega_{rs} \quad (4)$$
$$e_{bst} = f_{bst}(\theta_{ra}) \lambda_p \omega_{rs} \quad (5)$$
$$e_{cst} = f_{cst}(\theta_{ra}) \lambda_p \omega_{rs} \quad (6)$$

Functions $f_{ast}(\theta_{ra})$, $f_{bst}(\theta_{ra})$, and $f_{cst}(\theta_{ra})$ have direct relation with e_{ast}, e_{bst}, and e_{cst} therefore, these function have the same form as EMFs with peak value equal to ±1. The waveforms are devoid of sharp edges and are curved because they are related to flux linkages.

$$T_e = \lambda_p f_{ast}(\theta_{ra}) i_{ast} + f_{bst}(\theta_{ra}) i_{bst} + f_{cst}(\theta_{ra}) i_{cst} (N \cdot m) \quad (7)$$

The equation for mechanical parameters involving inertia J_m, coefficient of friction B_m along with load torque T_l with reference to rotor angle θ_{ra} and rotor speed ω_{rs} is given by

$$J_m \frac{d\omega_{rs}}{dt} + B_m \omega_{rs} = (T_e - T_l) \quad (8)$$

$$\frac{d\theta_{ra}}{dt} = \frac{p}{2} \omega_{rs} \quad (9)$$

Whereas, total poles in machine = p, Mechanical rotor speed (rad/s) = ω_{rs}, Rotor position in (rad)=θ_{ra}[1-5].

PM BLDC Motor parameters: Implements a three-phase permanent magnet Brushless Direct Current machine. The stator windings are connected in Star to an internal neutral point[5].

Table-1: BLDC Motor Model Parameter.

Parameters of BLDC Motor Drive	Symbols	Value
Power	P	3Hp
Resistance of Stator	R_s	0.2 Ω
Inductance of stator Phase	L_s	8.5mH
Flux linkage		0.175 V.s
Voltage Constant (DC)	V_{dc}	320 Volt
Torque Constant		1.4Nm
Viscous friction	B_m	0.005N.m.s
Inertia of Rotor	J_m	$0.089 kg.m^2$
Back-EMF Span (degree)		120^0
Number of pole pairs	p	4
Base speed	W_{base}	1650RPM

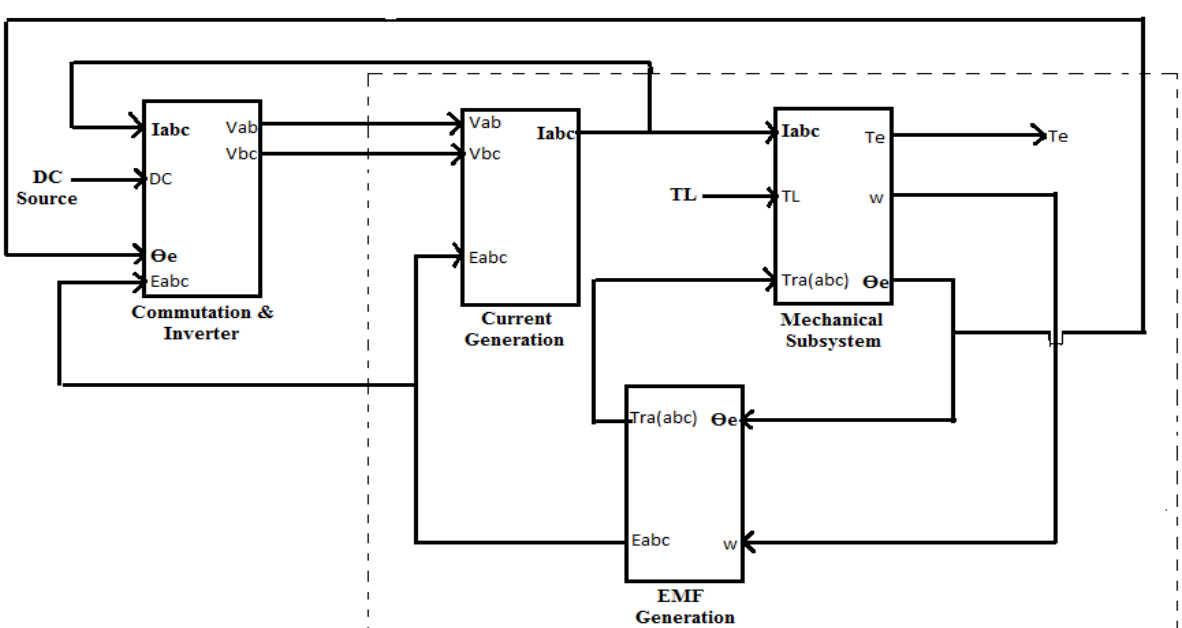

BLDC Motor

Figure-1: BLDC motor Block Diagram representation.

BLDC motor comprises of following sections: i. Current Generation, ii. EMF Generation, iii. Mechanical Subsystem.

The input of Current Generation block is V_{ab} and V_{bc} with back EMF (E_{abc}) of all three phases and the output is three phase I_{abc}.

This three-phase current (I_{abc}) is input for mechanical subsystem block. The other inputs are load torque (T_L) and trapezoidal EMF ($T_{ra(abc)}$). Trapezoidal EMF generated by EMF generation block. Output of mechanical subsystem is electrical torque (T_e), angular speed (ω) and electrical angle (θ_e).

Back EMF (E_{abc}) and trapezoidal EMF ($T_{ra(abc)}$) are formed by combination of angular speed (ω) and electrical angle (θ_e), this combination also is input for current generation.

Back EMF (E_{abc}) from EMF generation block, electrical angle (θ_e) from mechanical subsystem and three phase current (I_{abc}) from current generation block from input for commutation of inverter block and the output is V_{ab} and V_{bc} which itself is input for current generation block.

This block diagram forms close loop and BLDC motor is depend on the same.

Dynamic Simulation Results

The MATLAB codes based the speed controlled of BLDC motor drive systems. Fixing speed and torque to a set value, simulation of torque drive can be done.

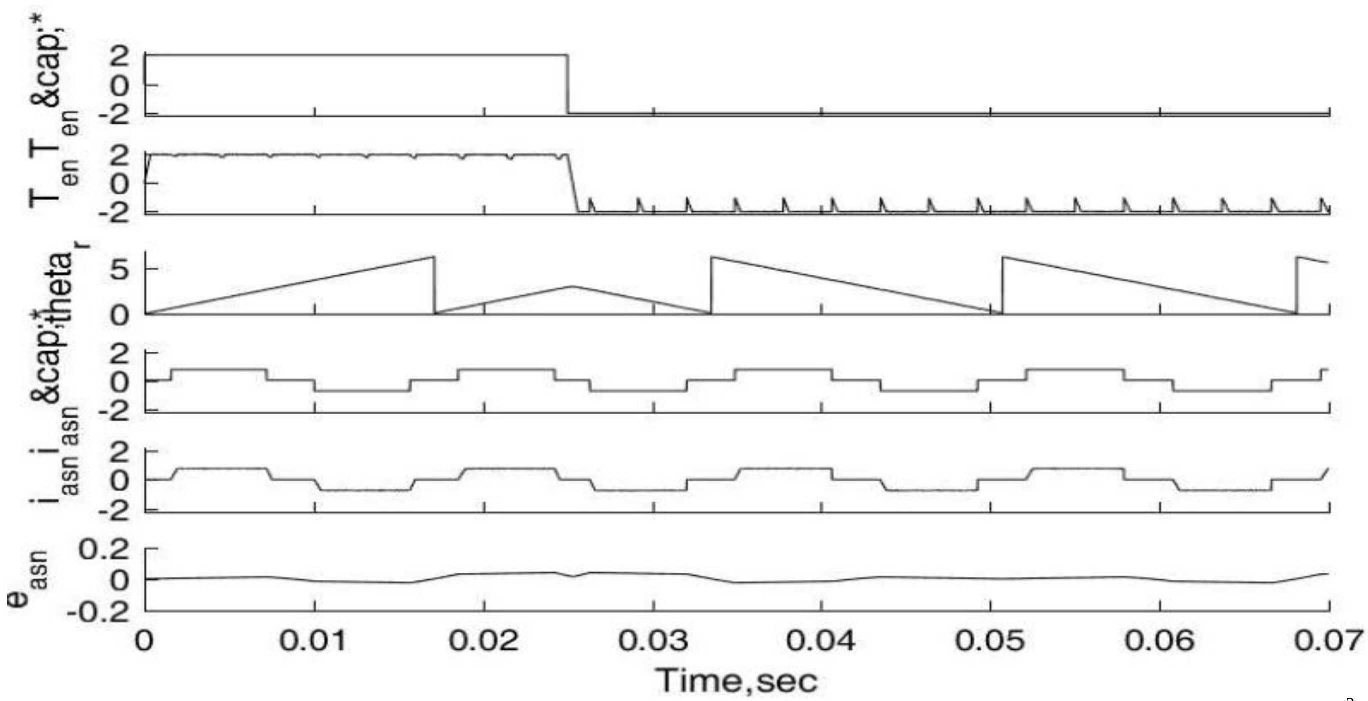

Figure-2: PM Brushless DC Motor speed controlled drive full wave Converter with standard inertia value J_m=0.089kg m^2 and Viscous friction value B_m= 0.005 Nms.

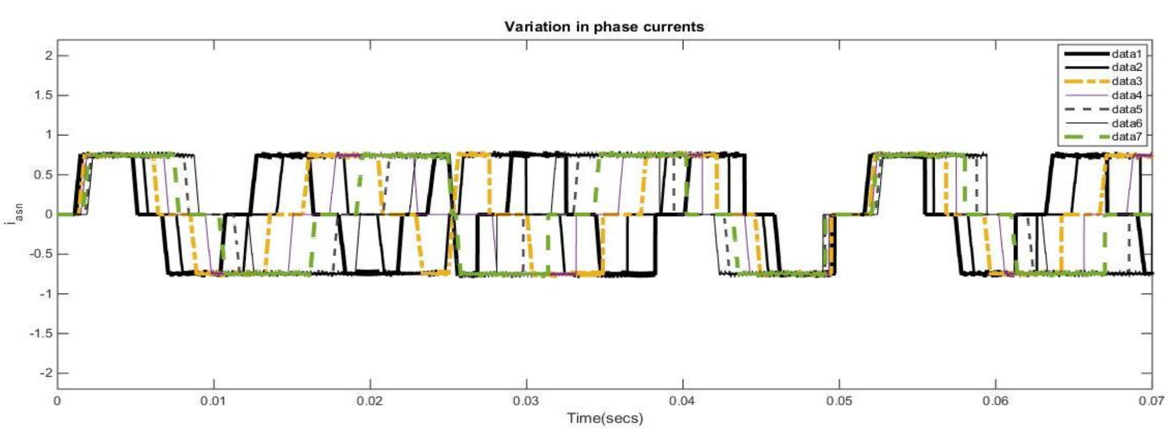

Figure-3: Effect of Change in inertia ± 30% on stator phase currents.

The description for legend as in the Change in motor inertia graph Data-1→ -30%, Data-2→ -20%, Data-3→ -10%, Data-4→ normal, Data-5→ +10%, Data-6→ +20%, Data-7→ +30%. With increase of inertia value from -30% of 0.089kg m^2 to +30% of 0.089kg m^2 corresponding increase in time period of stator current of BLDC motor is observed. With increase of inertia value from -30% of 0.089kg m^2 to +30% of 0.089kg m^2, rotor angle reaches particular angle more quickly. With increase of inertia value from -30% of 0.089kg m^2 to +30% of 0.089kg m^2 corresponding decrease of speed of BLDC motor is observed. Ther is negligible changes in torque when we vary rotor inertia value.

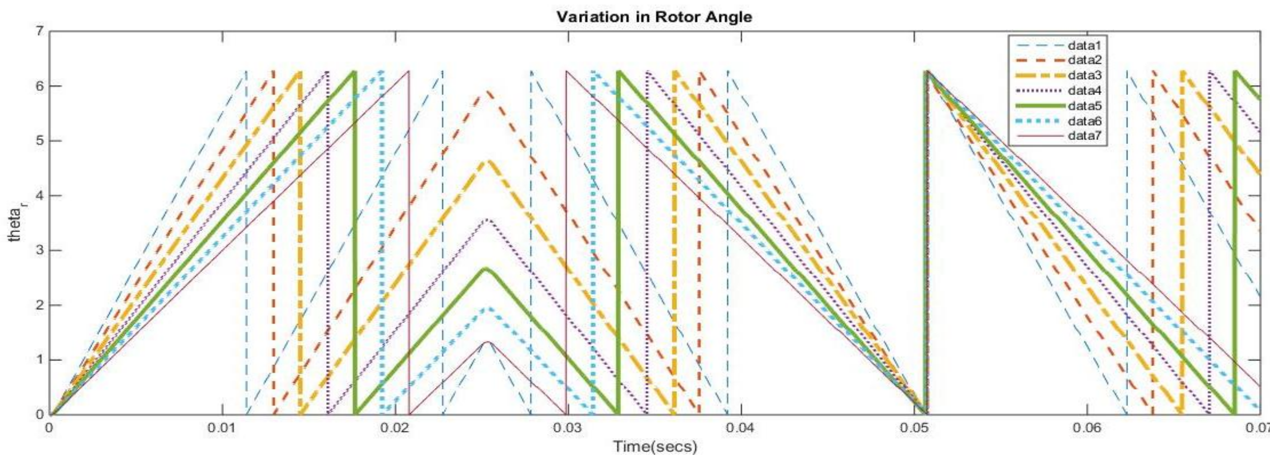

Figure-4: Effect of Change in inertia ±30% on rotor angle.

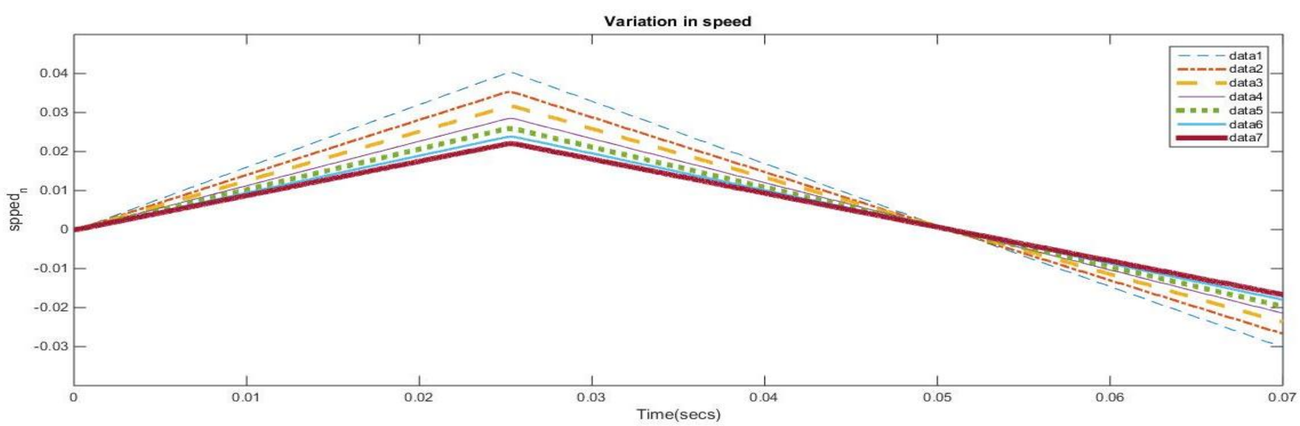

Figure-5: Effect of Change in inertia ±30% on rotor speed.

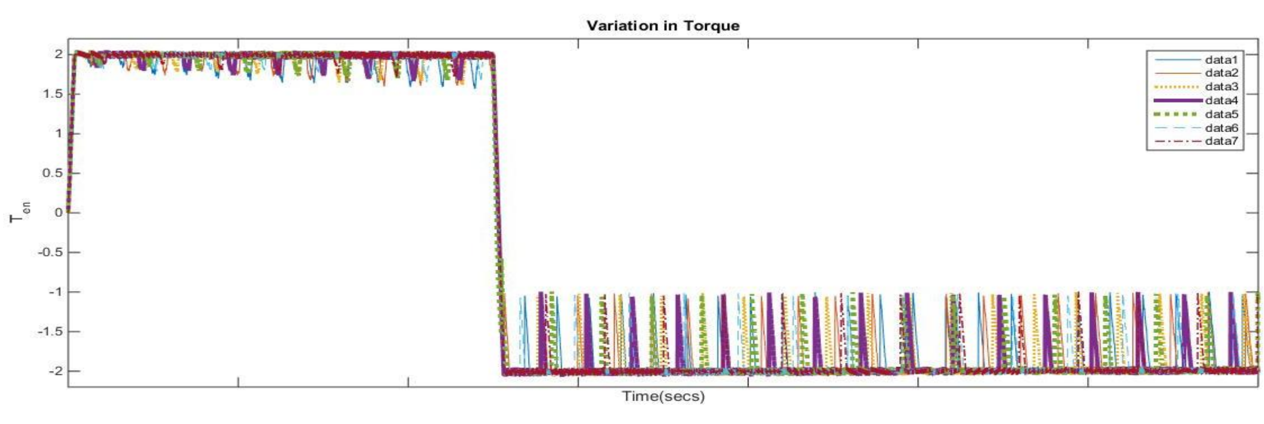

Figure-6: Effect of Change in inertia ±30% on Torque.

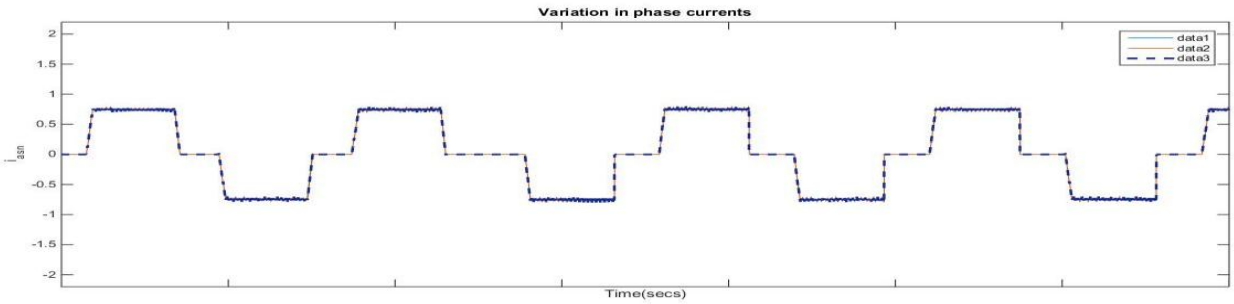

Figure-7: Effect of Change in Viscous friction ±20% on stator current.

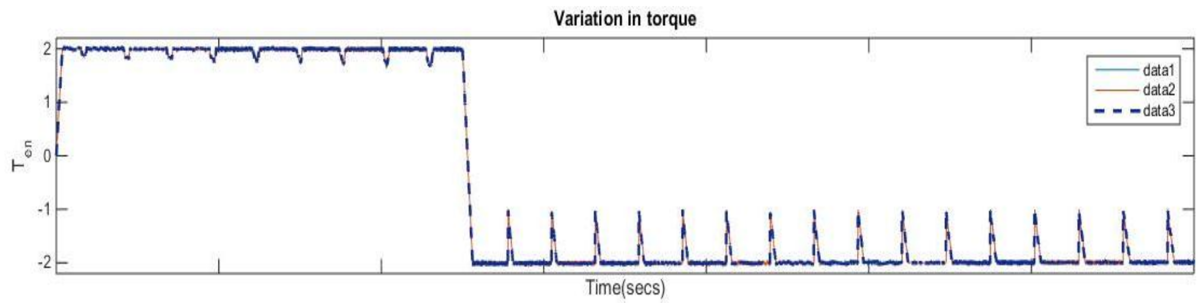

Figure-8: Effect of Change in Viscous friction ±20% on torque.

The description for legend as in the Change in Viscous friction graph Data -1→ -20%, Data -2→ normal, Data -3→ +20%.

Ther is no changes in stator current when we vary from -20% to +20% of viscous friction (0.005 N.m.s) value.

Ther is no changes in torque when we vary from -20% to +20% of viscous friction (0.005 N.m.s) value.

Conclusion

It is seen that when we take J_m = 0.089kg m^2 as a reference inertia and B_m=0.005N.m.s as a reference viscous friction value for comparison, it is observed that by increasing value of inertia, rotor angle increase and time period of stator current also increases with respect to time.

In this paper the simulation results for system mechanical parameter variation has also been obtained.

By observing waveform it is clearly understood that by changing inertia value and viscous friction in motor, changes in different parameters of motor is observed.

Simulation results clearly shows that parameter changes occur in rotor position, rotor speed, and stator current and back EMF. Rotor position reaches ‘0’ position or reference position quickly as we increase inertia value, where as time taken for completely one cycle for stator current increases and BEMF tends to becomes approx constant value.

These are the following changes that are observed with increase of motor inertia. Ther is no changes shown in stator current and torque when we varyviscous friction.

References

1. P. Pillay and R. Krishnan (1989). Modeling, simulation, and analysis of permanent- magnet motor drives. II. The brushless DC motor drive. *IEEE Transactions on Industry Applications*, 25(2), 274–279.
2. Kim T., Lee H. W. and Ehsani M. (2007). Position sensorless brushless DC motor /generator drives: review and future trends. *IET Electr. Power Appl*., 1(4), 557-564, 10.1049/iet-epa:20060358.
3. Krishnan R. and Rim G.H. (1990). Modeling, simulation, and analysis of variable-speed constant frequency power conversion scheme with a permanent magnet brushless dc generator. *IEEE Transactions on Industrial Electronics*, 37(4), 291–296.
4. Krishnan R. (2010). Permanent Magnet Synchronous and BrushlessDC Motor Drives, Electrical and Computer Engineering Department Virginia Tech Blacksburg, Virginia, U.S.A. Taylor and Francis Group, London New York.
5. Bhim Singh and Sanjeev Singh (2009). State of the Art on Permanent Magnet Brushless DC Motor Drives. *Journal of Power Electronics*, 9(1), DOI: 10.1.1.453.6253

6. Krishnan R. (2001). Electric Motor Drives. Prentice Hall, Upper Saddle River.

7. Saranya, R., kumar, S. S., Baskaran, R., & Vin, A. (2014). Sensorless Operation of Brushless DC Motor Drive using Back EMF Technique. *International Journal of Engineering Research*, 3(4), 255-257.

8. R. Krishnan, R. A. Bedingfi eld and A. S. Bharadwaj et al (1991). Design and development of a userfriendly PC-based CAE software for the analysis of torque/speed/position controlled PM brushless DC motor drive system dynamics. Conference Record, IEEE Industry Applications Society Annual Meeting (Cat. No. 91CH3077-5), 1388–1394.

9. Krishnan R. (2010). Permanent Magnet Synchronous and Brushless DC Motor Drives, Electrical and Computer Engineering Department Virginia Tech Blacksburg, Virginia. Taylor and Francis Group, London New York.

10. Debjyoti Chowdhurya, Madhurima Chattopadhyaya and Priyanka Roy (2013). Modelling and Simulation of Cost Effective Sensorless Drive for Brushless DC Motor. International Conference on Computational Intelligence: Modelling, Techniques and Applications ELSEVIER. DOI: 10.1016.

11. Rao, K. R., & Taib, S. (2008). Sensorless control of a BLDC motor with back EMF detection method using DSPIC. In 2008 IEEE 2nd International Power and Energy Conference. IEEE. pp. 243-248.

12. Ahirwal, B. K., Pandey, K. K., & Bhadoriya, J. S. (2014). A Novel Approach of Rotor Position Detection of a Sensorless BLDC Motor with Improved Back EMF. *Int. Journ. of Advanced Research in Electrical, Electronics and Instrumentation Engineering*, 3(11).

13. Safdarzadeh, O., Nezamabadi, M., & Afjei, E. (2016). A precise method to detect the accurate rotor position in BLDC motors at standstill condition. 7th Power Electronics and Drive Systems Technologies Conference (PEDSTC). IEEE. pp. 41-47.

14. Suganya, P., Priyadharshini, S., & Saranya, S. (2015). Sensorless control of a brushless DC motor. In National Conf. on Research Advances in Communication, Computation, Electrical Science and Structures.

15. Sadh, J. S. (2017). Sensorless zero back EMF method for in rotor position control of BLDC motor drive. *Research Journal of Engineering*, 6(7), 14-19.

16. Sadhak singh Juli, Bhusnur Surekha and Dubey S.P.(2020). Designing of Sensorless Brushless DC Motor: A Review, proceedings of national conference on emerging technologies in energy systems (NCETES-2020). 11 sept 2020.